

# Syntheses, Molecular Structures, Electrochemical Behavior, Theoretical Study, and Antitumor Activities of Organotin(IV) Complexes Containing 1-(4-Chlorophenyl)-1-cyclopentanecarboxylato Ligands

Xianmei Shang,<sup>†,‡</sup> Xianggao Meng,<sup>‡</sup> Elisabete C.B.A. Alegria,<sup>†,§</sup> Qingshan Li,<sup>||</sup> M.Fátima C. Guedes da Silva,<sup>†,⊥</sup> Maxim L. Kuznetsov,<sup>†</sup> and Armando J.L. Pombeiro<sup>\*,†</sup>

<sup>†</sup>Centro de Química Estrutural, Complexo I, Instituto Superior Técnico, Technical University of Lisbon, Av. Rovisco Pais, 1049-001 Lisbon, Portugal

<sup>‡</sup>Department of Chemistry, Central China Normal University, 430079 Wuhan, China

<sup>§</sup>Área Departamental de Engenharia Química, ISEL, R. Conselheiro Emídio Navarro, 1950-062 Lisbon, Portugal

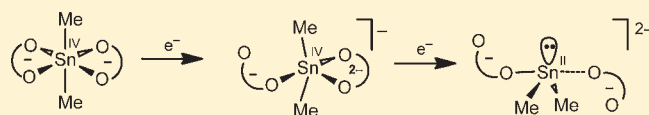
<sup>||</sup>School of Pharmaceutical Science, Shanxi Medical University, 86 South Xinjian Road, 030001 Taiyuan, China

<sup>⊥</sup>Universidade Lusófona de Humanidades e Tecnologias, ULHT Lisbon, Av. do Campo Grande, 376, 1749-024 Lisbon, Portugal

<sup>\*</sup>Tongji School of Pharmacy, Huazhong University of Science and Technology, 13 Hangkong Road, 430030 Wuhan, China

**S** Supporting Information

**ABSTRACT:** The organotin(IV) compounds [Me<sub>2</sub>Sn(L)<sub>2</sub>] (1), [Et<sub>2</sub>Sn(L)<sub>2</sub>] (2), [nBu<sub>2</sub>Sn(L)<sub>2</sub>] (3), [nOct<sub>2</sub>Sn(L)<sub>2</sub>] (4), [Ph<sub>2</sub>Sn(L)<sub>2</sub>] (5), and [PhOSnL]<sub>6</sub> (6) have been synthesized from the reactions of 1-(4-chlorophenyl)-1-cyclopentanecarboxylic acid (HL) with the corresponding diorganotin(IV) oxide or dichloride. They were characterized by IR and multinuclear NMR spectroscopies, elemental analysis, cyclic voltammetry, and, for 2, 3, 4 and 6, single crystal X-ray diffraction analysis. While 1–5 are mononuclear diorganotin(IV) compounds, the X-ray diffraction of 6 discloses a hexameric drumlike structure with a prismatic Sn<sub>6</sub>O<sub>6</sub> core. All these complexes undergo irreversible reductions and were screened for their *in vitro* antitumor activities toward HL-60, BGC-823, Bel-7402, and KB human cancer cell lines. Within the mononuclear compounds, the most active ones (3, 5) are easiest to reduce (least cathodic reduction potentials), while the least active ones (1, 4) are the most difficult to reduce. Structural rearrangements (*i.e.*, Sn–O bond cleavages and *trans*-to-*cis* isomerization) induced by reduction, which eventually can favor the bioactivity, are disclosed by theoretical/electrochemical studies.



## 1. INTRODUCTION

The potential of organotin(IV) compounds as biologically active metallopharmaceuticals has been recognized,<sup>1–24</sup> but their antitumor action mechanism is still unclear, although some evidence is consistent with their binding directly to DNA.<sup>25–28</sup> Investigations on metal-based drugs “activated by reduction” have become popular with platinum(IV) and ruthenium(III) compounds,<sup>29–35</sup> since various metal complexes can exist in rather inert high oxidation states in aqueous solution but are more labile and active in reduced oxidation states. It is believed that reduction to Pt(II) and Ru(II) is essential for the anticancer activity of many Pt(IV) and Ru(III) complexes.<sup>29–35</sup> Inspired by the reduction mechanism of these metal-based antitumor complexes, we decided to check if the reduction potential of organotin(IV) complexes could relate to their biological activity. To our knowledge, no well established information has yet been given on this matter.

Moreover, it is known that organotin(IV) carboxylates exhibit rather promising *in vitro* antitumor activities against

human tumor cell lines,<sup>1,18,19,36</sup> and that the presence of 4-chlorophenyl group can result in an enhanced activity of such complexes.<sup>18</sup> In the present work, we have selected a ligand, 1-(4-chlorophenyl)-1-cyclopentanecarboxylate (L<sup>−</sup>), which bears the 4-chlorophenyl group and a cycloalkyl ring connected to the carboxylate group and whose coordination chemistry and reactivity still remain almost unexplored. Moreover, the presence of the cycloalkyl moiety should increase the lipophilicity of the complex with expected promotion of cellular uptake and biological action.<sup>37,38</sup>

Hence, in this study we prepared six organotin(IV) complexes bearing that ligand (Figure 1) and various R<sub>2</sub>Sn groups and checked their *in vitro* cytotoxic activities against four different human cell lines [promyelocytic leukemia (HL-60), hepatocellular carcinoma (Bel-7402), nasopharyngeal carcinoma (KB), and gastric carcinoma (BGC-823)]. Moreover,

**Received:** March 28, 2011

**Published:** July 27, 2011

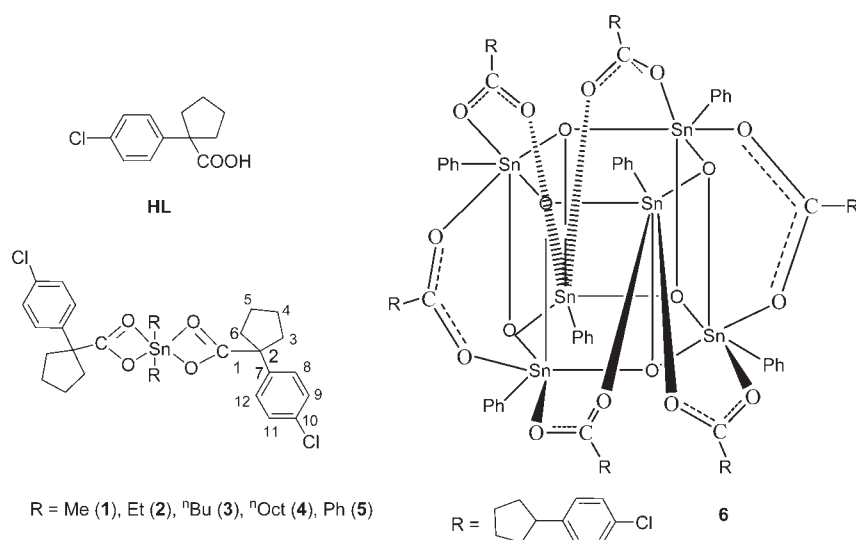


Figure 1. Structures of the ligand and complexes 1–6.

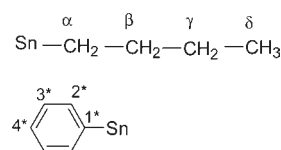
we performed cyclic voltammetric measurements of their reduction potential toward the eventual recognition of a redox potential–activity relationship.

Other main aims of this work, also with significance to the hypothesis of the mechanism of action by reduction are as follows: to get an insight into the reactions involved upon reduction of the Sn(IV) complexes (by performing theoretical calculations) which eventually could play a promoting role of the drug antitumor activity, a type of study that, to our knowledge, had not yet been applied to tin complexes.

## 2. EXPERIMENTAL SECTION

**2.1. General Remarks.** 1-(4-Chlorophenyl)-1-cyclopentanecarboxylic acid,  $[\text{Me}_2\text{SnCl}_2]$ ,  $[\text{Et}_2\text{SnCl}_2]$ ,  $[\text{nBu}_2\text{SnO}]$ ,  $[\text{nOct}_2\text{SnO}]$ ,  $[\text{Ph}_2\text{SnCl}_2]$ , and  $[\text{Ph}_2\text{SnO}]$  were purchased from Aldrich or Alfa and used as received. The other reagents were of analytical grade. C and H elemental analyses were carried out by the Microanalytical Service of the Instituto Superior Técnico. Infrared spectra ( $4000\text{--}400\text{ cm}^{-1}$ ) were recorded with a Biorad FTS 3000MX instrument in KBr pellets. The  $^1\text{H}$  and  $^{13}\text{C}$  ( $\text{Me}_4\text{Si}$  internal standard) and  $^{119}\text{Sn}$  ( $\text{Me}_4\text{Sn}$  external standard) NMR spectra were recorded on a Bruker Avance II+ 400 MHz (UltraShield Magnet) spectrometer. Electrochemical measurements were performed on an EG&G PAR273A potentiostat/galvanostat connected to a personal computer through a GPIB interface. Cyclic voltammograms (CV) were obtained using a two-compartment three-electrode cell, at Pt disk working ( $d = 1.0\text{ mm}$ ) and Pt wire counter electrodes, in  $0.2\text{ M } [\text{nBu}_4\text{N}][\text{BF}_4]/\text{THF}$  solution. Controlled-potential electrolyses (CPE) were carried out in electrolyte solutions with the above-mentioned composition, in a three-electrode H-type cell. The compartments were separated by a sintered glass frit and equipped with platinum gauze working and counter electrodes. For both CV and CPE experiments, a Luggin capillary connected to a silver wire pseudo-reference electrode was used to control the working electrode potential. The CPE experiments were monitored regularly by cyclic voltammetry (CV), thus assuring no significant potential drift occurred along the electrolyses. The redox potentials of the complexes were measured by CV in the presence of ferrocene as internal standard, and their values are quoted relative to the SCE by using the  $[\text{Fe}(\eta^5\text{-C}_5\text{H}_5)_2]^{0/+}$  ( $E_{1/2}^{\text{OX}} = 0.545\text{ vs SCE}$ ) redox couple in  $0.2\text{ M } [\text{nBu}_4\text{N}][\text{BF}_4]/\text{THF}$ .<sup>39</sup>

**2.2. Synthesis.** Atom labeling, used for NMR assignment, for  $\text{R} = \text{nBu}$ , Ph, follows:



**2.2.1. Synthesis of  $[\text{Me}_2\text{SnL}_2]$  (1).**  $[\text{Me}_2\text{SnCl}_2]$  (0.110 g, 0.50 mmol) was added to an undried methanolic solution (10 mL) of 1-(4-chlorophenyl)-1-cyclopentanecarboxylic acid (HL, 0.224 g, 1.0 mmol) and KOH (0.056 g, 1.0 mmol). The solution was stirred at room temperature overnight. Water (10 mL) was then added leading to the formation of a white precipitate of  $[\text{Me}_2\text{SnL}_2]$ , which was then separated by filtration, recrystallized from methanol, and dried *in vacuo*. Yield: 40%. Anal. Calcd for  $\text{C}_{26}\text{H}_{30}\text{Cl}_2\text{O}_4\text{Sn}$  (596.13): C 52.38, H 5.07. Found: C 52.11, H 5.24. IR (KBr): 2921, 1559 ( $\text{COO}_{\text{asym}}$ ), 1384 ( $\text{COO}_{\text{sym}}$ ), 580 (Sn–C), 431 (Sn–O)  $\text{cm}^{-1}$ .  $^1\text{H}$  NMR (400.0 MHz,  $\text{CDCl}_3$ ):  $\delta = 7.38$  (s, 4H, H-9, H-11), 7.27 (s, 4H, H-8, H-12), 1.80–1.70 (m, 16H, H-3, H-4, H-5, H-6), 0.42 (s, 3H, Sn- $\text{CH}_3$ ), 0.24 (s, 3H, Sn- $\text{CH}_3$ ).  $^{13}\text{C}$  NMR (100.6 MHz,  $\text{CDCl}_3$ ):  $\delta = 179.3$  (C-1); 144.1 (C-10), 132.2 (C-9, C-11), 128.2 (C-7, C-8, C-12), 36.2 (C-2), 23.6 (C-3, C-4, C-5, C-6), 8.1 (Sn- $\text{CH}_3$ ), 6.5 (Sn- $\text{CH}_3$ ).  $^{119}\text{Sn}$  NMR (149.2 MHz,  $\text{CDCl}_3$ ):  $\delta = -177.7$ .

**2.2.2. Synthesis of  $[\text{Et}_2\text{SnL}_2]$  (2).** Compound 2 was prepared by following the method and conditions described for 1 and using HL (0.224 g, 1.0 mmol) and  $[\text{Et}_2\text{SnCl}_2]$  (0.124 g, 0.50 mmol). The white product was recrystallized from ethanol and dried *in vacuo*. Yield: 38%. Anal. Calcd for  $\text{C}_{28}\text{H}_{34}\text{Cl}_2\text{O}_4\text{Sn}$  (624.14): C 53.88, H 5.49. Found: C 53.41, H 5.52. IR (KBr): 2954, 2872, 1565 ( $\text{COO}_{\text{asym}}$ ), 1365 ( $\text{COO}_{\text{sym}}$ ), 507 (Sn–C), 436 (Sn–O)  $\text{cm}^{-1}$ .  $^1\text{H}$  NMR (400.0 MHz,  $\text{CDCl}_3$ ):  $\delta = 7.38\text{--}7.27$  (m, 8H, H-8, H-9, H-11, H-12), 1.90–1.02 (m, 20H, H-3, H-4, H-5, H-6, Sn- $\text{CH}_2$ ), 0.84 (t,  $J = 7.6\text{ Hz}$ , 6H, 2 $\text{CH}_3$ ).  $^{13}\text{C}$  NMR (100.6 MHz,  $\text{CDCl}_3$ ):  $\delta = 186.4$  (C-1); 142.0 (C-10), 132.6 (C-5), 128.4 (C-9, C-11), 128.2 (C-8, C-12), 58.6 (C-2), 36.4 (C-3, C-6), 23.7 (C-4, C-5), 17.5 (Sn- $\text{CH}_2$ ), 8.5 (Sn- $\text{CH}_2\text{CH}_3$ ).  $^{119}\text{Sn}$  NMR (149.2 MHz,  $\text{CDCl}_3$ ):  $\delta = -163.3$ .

**2.2.3. Synthesis of  $[\text{nBu}_2\text{SnL}_2]$  (3).** Dibutyltin(IV) oxide (0.5 mmol) was added to a dry methanol/benzene (60 mL, 1:3 v/v) solution of HL (1.0 mmol) which was refluxed for 6 h. The solvent was then evaporated to dryness. The residue was recrystallized from ethanol and dried *in*

*vacuo*. Yield: 72%. Anal. Calcd for  $C_{32}H_{42}Cl_2O_4Sn$  (680.25): C 56.50, H 6.22. Found: C 56.72, H 6.40. IR (KBr): 2957, 2872, 1566 (COO<sub>asym</sub>), 1360 (COO<sub>sym</sub>), 510 (Sn–C), 436 (Sn–O)  $cm^{-1}$ .  $^1H$  NMR (400.0 MHz,  $CDCl_3$ ):  $\delta$  = 7.38–7.25 (m, 8H, H-8, H-9, H-11, H-12), 1.88–1.08 (m, 28H, H-3, H-4, H-5, H-6,  $\alpha$ -H,  $\beta$ -H,  $\gamma$ -H), 0.74 (t,  $J$  = 7.2 Hz, 6H,  $\delta$ -H).  $^{13}C$  NMR (100.6 MHz,  $CDCl_3$ ):  $\delta$  = 186.1 (C-1); 142.0 (C-10), 132.5 (C-5), 128.5 (C-9, C-11), 128.2 (C-8, C-12), 58.7 (C-2), 36.3 (C-3, C-6), 23.6 (C-4, C-5), 26.3 ( $\alpha$ -C,  $^1J$  ( $^{119}Sn$ – $^{13}C$ ) = 675 Hz), 26.0 ( $\beta$ -C), 24.9 ( $\gamma$ -C), 13.4 ( $\delta$ -C).  $^{119}Sn$  NMR (149.2 MHz,  $CDCl_3$ ):  $\delta$  = –156.7.

**2.2.4. Synthesis of [ $^{19}Oct_2SnL_2$ ] (4).** Dioctyltin(IV) oxide (0.5 mmol) was added to a dry methanol/benzene (60 mL, 1:3 v/v) solution of HL (1.0 mmol) which was refluxed for 6 h. The solvent was then evaporated to dryness. The residue was recrystallized from methanol/*n*-hexane and dried *in vacuo*. Yield: 66%. Anal. Calcd for  $C_{40}H_{58}Cl_2O_4Sn \cdot 2CH_3OH$  (856.59): C 58.89, H 7.77. Found: C 58.89, H 8.03. IR (KBr): 2924, 2853, 1566 (COO<sub>asym</sub>), 1368 (COO<sub>sym</sub>), 512 (Sn–C), 435 (Sn–O)  $cm^{-1}$ .  $^1H$  NMR (400.1 MHz,  $CDCl_3$ ):  $\delta$  = 7.38–7.26 (m, 8H, H-8, H-9, H-11, H-12), 1.88–1.10 (brm, 44H, H-3, H-4, H-5, H-6, Sn-(CH<sub>2</sub>)<sub>7</sub>), 0.91 (m, 6H, 2CH<sub>3</sub>).  $^{13}C$  NMR (100.6 MHz,  $CDCl_3$ ):  $\delta$  = 186.2 (C-1); 142.3 (C-10), 132.7 (C-5), 128.4 (C-9, C-11), 128.2 (C-8, C-12), 58.6 (C-2), 36.3, 33.1, 31.8, 29.1, 29.0, 25.1, 24.3, 23.6, 22.6 (C-3, C-4, C-5, C-6, Sn-(CH<sub>2</sub>)<sub>7</sub>), 14.1 (CH<sub>3</sub>).  $^{119}Sn$  NMR (149.2 MHz,  $CDCl_3$ ):  $\delta$  = –157.2.

**2.2.5. Synthesis of [ $Ph_2SnL_2$ ] (5).** Diphenyltin(IV) oxide (0.5 mmol) was added to a dry methanol/benzene (60 mL, 1:3 v/v) solution of HL (1.0 mmol) which was refluxed for 6 h. The solvent was then evaporated to dryness. The residue was recrystallized from benzene and dried *in vacuo*. Yield: 66%. Anal. Calcd for  $C_{36}H_{34}Cl_2O_4Sn$  (720.27): C 60.03, H 4.76. Found: C 60.12, H 4.70. IR (KBr): 1522 (COO<sub>asym</sub>), 1394 (COO<sub>sym</sub>), 517 (Sn–C), 404 (Sn–O)  $cm^{-1}$ .  $^1H$  NMR (400.1 MHz,  $CDCl_3$ ):  $\delta$  = 7.35–7.24 (m, 18H, H-8, H-9, H-11, H-12, H-2\*, H-3\*, H-4\*), 2.74–2.70, 1.91–1.61 (m, 16H, H-3, H-4, H-5, H-6).  $^{13}C$  NMR (100.6 MHz,  $CDCl_3$ ):  $\delta$  = 180.4 (C-1), 141.5 (C-10), 138.2 (C-1\*), 136.6, 135.1, 130.5, 128.8 (C-2\*, C-3\*, C-4\*, C-7, C-8, C-9, C-11, C-12), 58.7 (C-2), 36.3, 23.6 (C-3, C-4, C-5, C-6).  $^{119}Sn$  NMR (149.2 MHz,  $CDCl_3$ ):  $\delta$  = –320.5.

**2.2.6. Synthesis of [ $PhSnOL$ ]<sub>6</sub> (6).** A solution of HL (1.0 mmol) in ethanol (25 mL) was added to a solution of [ $Ph_2SnCl_2$ ] (344 mg, 1.0 mmol) in 25 mL of ethanol. The reaction mixture was stirred at 25 °C for 6 h. The solution was filtered and left to slow evaporation at room temperature. Colorless crystals were formed from this solution after 6 d, washed with *n*-hexane, and dried *in vacuo*. Yield: 55%. Anal. Calcd for  $C_{108}H_{102}Cl_6O_{18}Sn_6 \cdot C_6H_{14}$  (2699.12): C 50.73, H 4.33. Found: C 50.67, H 3.70. IR (KBr): 1589 (COO<sub>asym</sub>), 1398 (COO<sub>sym</sub>), 729, 623, 559, 499, 438  $cm^{-1}$ .  $^1H$  NMR (400.1 MHz,  $CDCl_3$ ):  $\delta$  = 7.40–6.67 (m, 54H, H-8, H-9, H-11, H-12, H-2\*, H-3\*, H-4\*), 2.51–2.48, 2.40–2.37, 1.79–1.74, 1.64–1.57 (m, 48H, H-3, H-4, H-5, H-6).  $^{13}C$  NMR (100.6 MHz,  $CDCl_3$ ):  $\delta$  = 184.1 (C-1); 143.3 (C-10), 143.3 (C-1\*), 141.3 (C-2\*), 140.8 (C-3\*), 134.2 (C-4\*), 128.4 (C-7), 128.0 (C-9, C-11), 127.9 (C-8, C-12), 60.3 (C-2), 36.8, 31.5 (C-3, C-6), 23.5, 23.3, 22.6, 14.1 (C-4, C-5).  $^{119}Sn$  NMR (149.2 MHz,  $CDCl_3$ ):  $\delta$  = –541.1.

**2.3. Structural Determination and Refinement.** Suitable single crystals of the complexes were mounted in glass capillaries for X-ray structural analysis. Intensity data were collected at room temperature, using a Bruker AXS-KAPPA APEX II diffractometer with graphite monochromated Mo K $\alpha$  ( $\lambda$  0.710 73 Å) radiation. Cell parameters were retrieved using Bruker SMART software and refined using Bruker SAINT<sup>40</sup> on all the observed reflections. Absorption corrections were applied using SADABS.<sup>38</sup> Structures were solved by direct methods by using the SHELXS-97 package<sup>41</sup> and refined with SHELXL-97.<sup>42</sup> Calculations were performed using the WinGX System-Version 1.80.03.<sup>43</sup> All hydrogen atoms were inserted in calculated positions. Least-squares refinements with anisotropic thermal motion

parameters for all the non-hydrogen atoms and isotropic for the remaining atoms were employed.

Crystal data and refinement parameters are shown in Table S1, Supporting Information. CCDC numbers 783753–783756 contain the supplementary crystallographic data for this paper. These data can be obtained free of charge from the Cambridge Crystallographic Data Centre via [www.ccdc.cam.ac.uk/datarequest/cif](http://www.ccdc.cam.ac.uk/datarequest/cif).

**2.4. Cytotoxicity Study.** The following human cell lines were used for screening: promyelocytic leukemia (HL-60), hepatocellular carcinoma (BEL-7402), gastric carcinoma (BGC-823), and nasopharyngeal carcinoma (KB) cell lines. All of them were grown and maintained in RPMI-1640 medium supplemented with 10% fetal bovine serum, penicillin (100 U/mL), and streptomycin (100  $\mu$ g/mL) at 37 °C in humidified incubators in an atmosphere of 5% CO<sub>2</sub>.

Cell proliferation in compound-treated cultures was evaluated by using a system based on the tetrazolium compound (MTT)<sup>44</sup> and sulforhodamine B (SRB) methods<sup>45</sup> in the State Key Laboratory of Natural and Biomimetic Drugs, Beijing Medical University (China). All cell lines were seeded into 96 well plates at a concentration of about 50 000 cells/mL and were incubated in an atmosphere of 5% CO<sub>2</sub> for 24 h. Then, 20  $\mu$ L of the sample (organotin complex) were added, and further incubation was carried out at 37 °C for 48 h. To prepare these samples of the complexes, they were first dissolved in DMSO at a concentration of 10<sup>–1</sup> M and diluted with medium to concentrations between 10<sup>–4</sup> and 10<sup>–6</sup> M. The final concentration of DMSO was less than 1%, and at this concentration it did not affect cell growth.<sup>46</sup> A 50  $\mu$ L portion of 0.1% MTT or SRB (Sigma) was added to each well. After 4 h incubation, the culture medium was removed, and 150  $\mu$ L of isopropanol were added to dissolve the insoluble blue formazan precipitates produced by MTT reduction. The plate was shaken for 20 min on a plate shaker to ensure complete dissolution. The optical density of each well was measured at 570 nm (MTT) or 540 nm (SRB) wavelengths. The antitumor activity was determined three times in independent experiments, using four replicate wells per toxicant concentration (10, 1, 0.1  $\mu$ M), and the mean optical densities for drug-treated cells at each concentration were obtained as a percentage of that of untreated cells.

**2.5. Computational Details.** The full geometry optimization of the complexes has been carried out in Cartesian coordinates at the DFT/HF hybrid level of theory using Becke's three-parameter exchange functional<sup>47</sup> in combination with the gradient-corrected correlation functional of Lee, Yang, and Parr<sup>48</sup> (B3LYP) with the help of the Gaussian-98<sup>49</sup> program package. The restricted approximation for structure **1** with closed electron shells and the unrestricted method for the reduced complexes **1<sup>–</sup>** and **1<sup>2–</sup>** have been employed. For the doubly reduced species **1<sup>2–</sup>**, both singlet and triplet spin states have been calculated, and the former one was found as the ground state. Symmetry operations were not applied for all structures. A quasirelativistic Stuttgart pseudopotential described 46 core electrons, and the corresponding basis set<sup>50</sup> for the tin atom and the 6-31G(d) basis set for other atoms were used. The Hessian matrix was calculated analytically to prove the location of correct minima (no imaginary frequencies were found) and to estimate the thermodynamic parameters, the latter being calculated at 25 °C. The electronic structures of **1<sup>–</sup>** and **1<sup>2–</sup>** were additionally examined using the natural bond orbital (NBO) analysis.<sup>51</sup> The experimental X-ray geometry of **2** was taken as a basis for the initial geometry of the optimization processes.

## 3. RESULTS AND DISCUSSION

**3.1. Syntheses.** The 1:2 alkyltin(IV) substituted cyclopentanecarboxylates [ $R_2SnL_2$ ] **1–2** (R = Me and Et) were obtained by reaction of the appropriate dialkyltin(IV) dichloride, in an undried methanolic solution, with 1-(4-chlorophenyl)-1-cyclopentanecarboxylic acid (HL) and KOH (both in a 2-fold molar

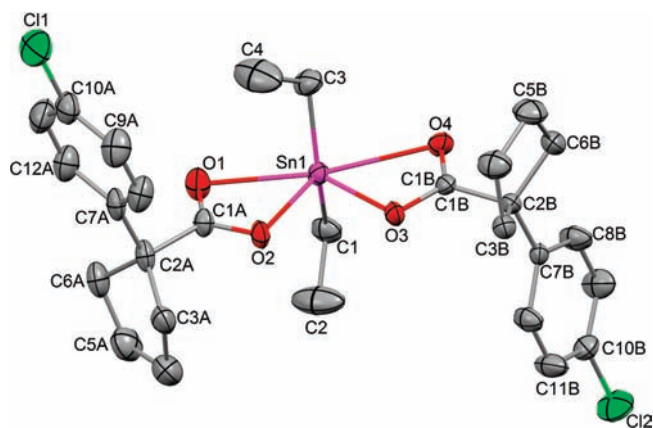


**Figure 2.** Crystal structure of **2** with atomic numbering scheme (hydrogen atoms are omitted for clarity). Atoms drawn at 30% probability. Selected bond lengths (Å) and angles (deg): Sn1–C1 2.096(5), Sn1–C3 2.110(5); Sn1–O1 2.497(3), Sn1–O2 2.126(2), Sn1–O3 2.129(3), C1A–O1 1.246(5), C1A–O2 1.281(5); C1–Sn1–C3 150.6(2), C1–Sn1–O2 101.59(14), C3–Sn1–O2 102.03(15), C1–Sn1–O3 100.33(16), C3–Sn1–O3 99.92(17), O2–Sn1–O3 82.30(10), C1–Sn1–O1 88.37(16), C3–Sn1–O1 90.66(16), O2–Sn1–O1 55.72(10), O3–Sn1–O1 138.01(9), C2–C1–Sn1 116.1(4).

amount relatively to the tin complex), while the compounds **3–5** (R = <sup>n</sup>Bu, <sup>n</sup>Oct and Ph) were synthesized by reaction of HL with di-*n*-butyltin (di-*n*-octyltin or diphenyltin) oxide in dry methanol/benzene (1:3, v/v). The *drum* (see below) phenyltin(IV) complex [PhSnOL]<sub>6</sub> **6** was produced by reaction of [Ph<sub>2</sub>SnCl<sub>2</sub>] with HL in ethanol solution at room temperature.

The complexes were isolated as white solids in moderate to good (40–72%) yields. They are stable in air, insoluble in water, and soluble in chloroform, acetone, DMSO, and mixtures of water/DMSO. The complexes with ethyl, *n*-butyl, *n*-octyl, and phenyl groups tend to exhibit higher solubility in organic solvents than that with methyl groups. The complexes were characterized by FT-IR, <sup>1</sup>H, <sup>13</sup>C, <sup>119</sup>Sn NMR spectroscopies and elemental analysis, as well as by single-crystal X-ray diffraction analysis for [Et<sub>2</sub>SnL<sub>2</sub>] (**2**), [<sup>n</sup>Bu<sub>2</sub>SnL<sub>2</sub>] (**3**), [<sup>n</sup>Oct<sub>2</sub>SnL<sub>2</sub>] (**4**), and [PhSnOL]<sub>6</sub> (**6**), representing the two types of diorganotin(IV) substituted cyclopentanecarboxylates.

**3.2. Spectroscopic Data.** The assignments of IR bands for all the complexes were done by comparing with the IR spectra of the free acid and related organotin compounds. 1-(4-Chlorophenyl)-1-cyclopentanecarboxylic acid displays a band at 1695 cm<sup>-1</sup> which is assigned to the ν(OCO)<sub>asym</sub> stretching vibration. The considerable shift of this vibration upon coordination in the organotin(IV) complexes is due to the binding to the metal through the carbonyl oxygen atom.<sup>52</sup> The criterion of the separation between the symmetric and asymmetric stretching wavenumbers of the carboxylate moiety, Δ = [ν(OCO)<sub>asym</sub> – ν(OCO)<sub>sym</sub>], has been applied to ascertain its bidentate/chelation or monodentate coordination type.<sup>53</sup> Although a clear line between the two categories cannot be drawn, values lower than 240 cm<sup>-1</sup> can be indicative of bidenticity and those higher than 260 cm<sup>-1</sup> point out monodenticity.<sup>54</sup> The observed values for all the compounds of this work are in the 128–206 cm<sup>-1</sup> range (the smallest value found in **5** and the highest one in **3**) indicating a bidentate mode of the ligand. This is in agreement with X-ray crystallography results (see below) which disclose such a type of coordination with a bridging interaction.

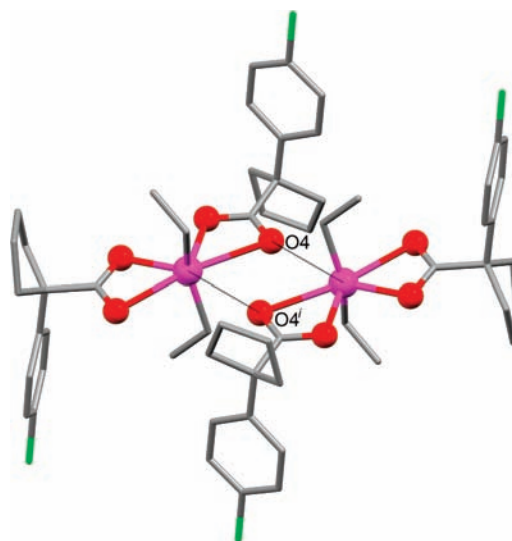


**Figure 3.** Structural representation of **2** showing the linkage of neighboring tin(IV) molecules via intermolecular Sn...O contact interactions, generating distorted pentagonal bipyramidal dinuclear aggregates. H atoms are omitted for clarity.

The <sup>1</sup>H and <sup>13</sup>C NMR data of complexes **1–6** are given in the Experimental Section (2.2), and the observed resonances have been assigned on the basis of their integration and coupling constants. The different R groups (Me, Et, <sup>n</sup>Bu, <sup>n</sup>Oct, Ph) attached to the tin atom gave signals in the expected region. The <sup>119</sup>Sn NMR resonances of complexes **1–4** occur at chemical shifts in the δ –156 to –177 range, while those for **5** and **6** are markedly shifted upfield (δ –320.5 and –541.1, respectively). According to the X-ray diffraction data (see the following section) all the compounds are six-coordinate with the possibility for heptacoordination in **1–5** if the species are visualized as oxygen-bridged dimers. According to examples found in the literature,<sup>55–59</sup> those values are acceptable for five-, six-, or even seven-coordinate tin(IV) compounds. Therefore, on the basis of <sup>119</sup>Sn NMR data alone, we cannot ascertain the geometry of the complexes in solution.

**3.3. X-ray Diffraction Analysis.** The molecular structures of the complexes **2, 3, 4**, and **6** were authenticated by single-crystal X-ray diffraction analyses. Selected experimental information is given in Table S1, and a summary of the most relevant bond distances and angles is given in the legends of Figures 2, S1, and S2.

The structures of complexes **2–4** (Figures 2 for complex **2**; Figures S1 and S2 for **3** and **4**, respectively) are quite similar. They are monomeric with the tin atoms in skewed trapezoidal bipyramidal environments formed by four O atoms derived from two carboxylates in the equatorial positions and two C atoms of the alkyl groups in the apical (*trans*) positions. However, these complexes also feature 2-fold linkages of neighboring units via intermolecular contacts, giving rise to the formation of dimeric tin aggregates (Figure 3). In such a situation, each tin metal can be considered as taking up a pentagonal bipyramid geometry where the intermolecular Sn...O bond distances assume values of 2.971(3) (**2**), 3.0026(19) (**3**), and 3.038(5) (**4**) Å. The carboxylate groups coordinate in an asymmetric mode forming both short and long Sn–O bonds as observed in other tin(IV) complexes.<sup>60,61</sup>

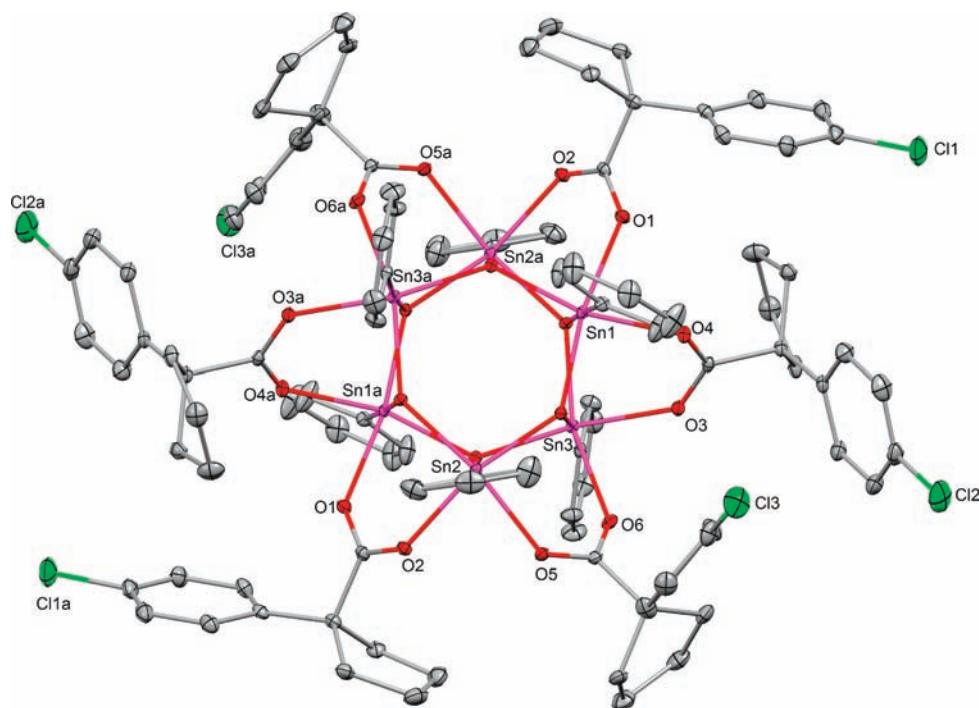


**Figure 4.** Molecular structure of **6**. For clarity, atoms are drawn at 10% probability, hydrogen atoms are omitted and only the labels of tin, chlorides, and some of the oxygen atoms are included. Selected bond lengths (Å) and angles (deg): Sn1–O1 2.136(3), Sn2–O2 2.173(3), Sn3–O3 2.164(3), Sn1–O4 2.153(2), Sn2–O5 2.175(2); O7–Sn1–O9a 104.77(10), O7–Sn1–O8 78.14(9), O9a–Sn1–O8 77.92(9), O7–Sn1–C37 100.98(13), O9a–Sn1–C37 104.65(12), O8–Sn1–C37 177.43(12), O7–Sn1–O1 162.13(10), O9a–Sn1–O1 84.22(10), O8–Sn1–O1 88.97(10), C37–Sn1–O1 91.36(13), O7–Sn1–O4 88.89(10), O9–Sn1–O4 155.65(10), O8–Sn1–O4 85.52(9), C37–Sn1–O4 92.06(13), O1–Sn1–O4 77.70(11). Symmetry operation to generate equivalent atoms: (a)  $1 - x, 2 - y, 1 - z$ .

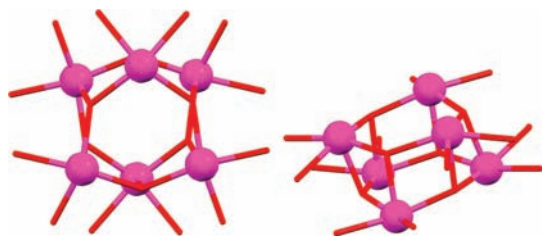


**Figure 5.** Perspective representations (arbitrary views) of the central *drum*-type tin–oxygen core in **6**.

The interesting structure of compound **6** (Figure 4) comprises a  $\text{Sn}_6\text{O}_6$  core and belongs to the known family of *drum* compounds among organostannoxanes.<sup>62–64</sup> The  $\text{Sn}_6\text{O}_6$  core contains two fused  $\text{Sn}_3\text{O}_3$  (the basal hexagonal faces of the *drum*) and  $\text{Sn}_2\text{O}_2$  four-membered rings forming the six lateral faces of the *drum* (Figure 5). All tin atoms are six-coordinate and held together by six L anions on the periphery which bridge, through isobidentate carboxylate moieties, alternate Sn atoms. The tin-coordinated phenyl rings are displayed above and below the hexagonal faces of the *drum*. Relevant intermolecular hydrogen bonds could also be found in this structure. Indeed, while the C1 > C6 phenyl centroids of L act as acceptors of the phenyl H50 of the nearest molecules [ $d(\text{H} \cdots \text{centroid})$  2.629 Å], thus expanding the structure along the crystallographic  $\alpha$  axis, the Cl2 chloride atoms act as acceptors of the phenyl H40 hydrogen atoms of vicinal molecules [ $d(\text{H} \cdots \text{Cl})$  2.921 Å] expanding the structure to a second dimension.

**Table 1.** Cyclic Voltammetric Data<sup>a</sup> for Complexes **1–6**, Free HL, and Chlorobenzene (PhCl)

compd	$E_p^{\text{red}}$ ( $I^{\text{red}}$ )	$E_p^{\text{ox}}$ ( $I^{\text{ox}}$ ) <sup>b</sup>	$E_p^{\text{ox}}$ ( $\Pi^{\text{ox}}$ ) <sup>b</sup>	$E_p^{\text{ox}}$ (HL, PhCl) <sup>b</sup>
<b>1</b>	−1.18	0.17	0.71	
<b>2</b>	−1.12	0.14	0.65	
<b>3</b>	−1.04	0.09	0.55	
<b>4</b>	−1.32		0.78	
<b>5</b>	−0.99	0.05	0.57	
<b>6</b>	−0.94		0.53	
HL <sup>c</sup>	−1.43			0.98
chlorobenzene <sup>c</sup>	−0.85			0.34

<sup>a</sup> Values in V  $\pm$  0.04 relative to SCE measured in 0.2 M [<sup>n</sup>Bu<sub>4</sub>N][BF<sub>4</sub>]/THF solution ( $\nu = 200 \text{ mVs}^{-1}$ ). Complex concentrations: 1.4–2.9 mM.

<sup>b</sup> Detected only upon scan reversal following the cathodic wave.

<sup>c</sup> Included for comparative purposes.

**3.4. Electrochemical and Theoretical Studies.** The redox properties of compounds **1–6**, as well as, for comparative purposes, of 1-(4-chlorophenyl)-1-cyclopentanecarboxylic acid (HL) and chlorobenzene, have been investigated by cyclic voltammetry (CV), at a Pt electrode ( $d = 1 \text{ mm}$ ) in 0.2 M [<sup>n</sup>Bu<sub>4</sub>N][BF<sub>4</sub>]/THF solution, at 25 °C, and the measured redox potentials (in V vs. SCE) are given in Table 1. The tin(IV) complexes show a two-electron (as confirmed by controlled-potential electrolysis) irreversible reduction process (broad wave  $I^{\text{red}}$ ) at  $E_p^{\text{red}}$  in the range from *ca.* −0.9 to −1.3 V vs SCE (Figure 6, for complex **1**). Moreover, upon scan reversal

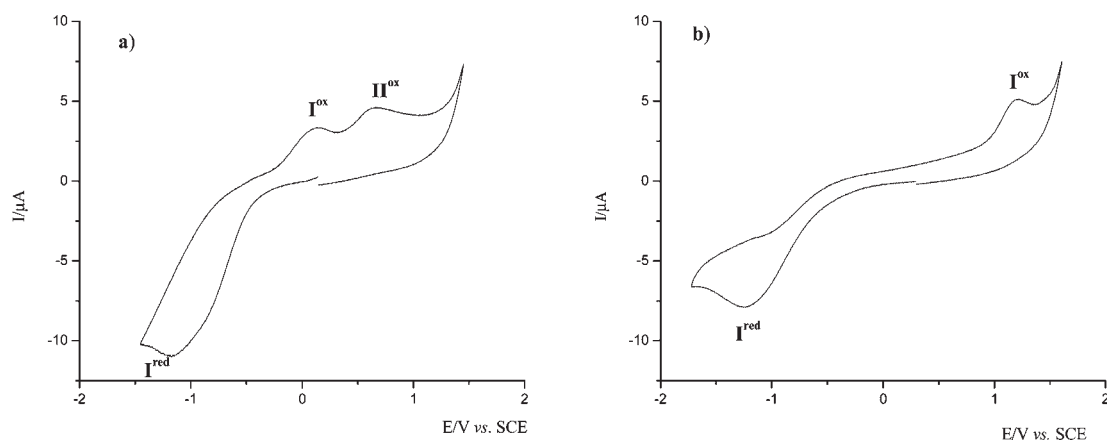


**Figure 6.** Cyclic voltammograms of complex **1** (a) and HL (b), initiated by the cathodic sweep, at a Pt electrode, in 0.2 M [ $n\text{Bu}_4\text{N}$ ][ $\text{BF}_4$ ]/THF solution ( $\nu = 200$  mV/s). [ $\text{Complex}$ ] = 1.4 mM; [ $\text{HL}$ ] = 3.9 mM.

after the reduction wave, one or two irreversible oxidation processes are detected at  $E_p^{\text{ox}}$  in the ranges of *ca.* 0.1–0.2 (wave  $\text{I}^{\text{ox}}$ ) and *ca.* 0.5–0.8 (wave  $\text{II}^{\text{ox}}$ ) V vs SCE. These oxidations concern species formed at the cathodic wave.

In accord with the weaker electron-donor character of phenyl relatively to alkyl groups, the reduction potential values for the phenyl complexes **5** and **6** (−0.99 and −0.94 V vs SCE, respectively) are less cathodic than those of the alkyl complexes **1**–**4**. The dependence of the redox potential of a complex on the electronic properties of its ligands has been well documented.<sup>65–74</sup>

Somehow related behaviors, under similar conditions, are exhibited by the free ligand itself in the neutral protonated form (1-(4-chlorophenyl)-1-cyclopentanecarboxylic acid, HL) and by chlorobenzene; i.e., they undergo a single-electron irreversible reduction process at −1.43 (HL) and −0.85 (PhCl) V vs SCE followed by an anodic wave at  $E_p^{\text{ox}} = 0.98$  (HL) and 0.34 (PhCl) V vs SCE upon potential scan reversal. However, despite the analogies, which suggest that the reduction of the complexes can be ligand centered, the electrochemical study cannot establish unambiguously which site(s) of the molecule (the  $\text{L}^-$  ligand or/and the metal center) is (are) involved in the reduction and become more affected. To clarify this situation and to interpret the electrochemical behavior of the [ $\text{R}_2\text{SnL}_2$ ] complexes, quantum-chemical calculations of the complex **1** and the corresponding singly and doubly reduced species  $\text{I}^-$  and  $\text{I}^{2-}$  have been carried out at the DFT (B3LYP) level of theory.

The calculated structural parameters of **1** (herein denoted by *trans-1*) are in good agreement with the experimental X-ray data for the similar complex **2** (denoted by *trans-2*). The maximum deviation was found for the Sn–C bonds (0.033–0.047 Å) and does not exceed 0.03 Å for the other bonds, often lying within the  $3\sigma$  interval of the experimental data. The analysis of the frontier MO composition indicates that the LUMO of *trans-1* is centered on the phenyl moiety and the carboxylate group of both ligands  $\text{L}^-$  with no involvement of the metal orbitals (Figure 7).

The geometry optimization of the singly reduced complex led to the cleavage of the Sn–O(4) bond to give  $\text{1a}^-$ . As a result, one of the  $\text{L}^-$  ligands in  $\text{1a}^-$  acquired a monodentate coordination mode while the other one remains bidentate (Figure S3). The spin density in  $\text{1a}^-$  is localized on the carboxylate group (mostly

at the C(1A) atom) and the Ph ring (the C(10A) and C(7A) atoms) of the bidentate  $\text{L}^-$  ligand. This is confirmed by the composition of the single occupied MO (SOMO) (Figure 7) and the natural bond orbital (NBO) analysis (the  $\alpha$  spin-NBO corresponding to the unpaired electron on the C(1A) atom was found with the occupancy of 0.81 e and the  $sp^{4.67}$  hybridization type). Thus, the one-electron reduction affects both the  $\text{L}^-$  ligands, one of them becoming monodentate and the other one remaining bidentate but acquiring the excess negative charge (Scheme 1, first step).

The LUMO of  $\text{1a}^-$  (130  $\alpha$ -MO and 129  $\beta$ -MO) is localized on the Ph group of the nonreduced monodentate ligand  $\text{L}^-$  (Figure 7). However, the *two-electron* reduction of *trans-1* affects the Sn atom rather than the ligands  $\text{L}^-$ , lowering the metal oxidation state from +IV in *trans-1* to +II in  $\text{I}^{2-}$  (Scheme 1, first and second steps). Indeed, the geometry optimization of the doubly reduced species resulted in the location of the equilibrium structure  $\text{I}^{2-}$ . Complex  $\text{I}^{2-}$  has the coordination polyhedron of a sawhorse (seesaw) type with two monodentate ligands  $\text{L}^-$  and the Me ligands tending to a *cis* position (C–Sn–C angle of *ca.* 95°), thus structurally differing markedly from *trans-1* (Figure S3). Such a structural type as well as the HOMO composition of  $\text{I}^{2-}$  (Figure 7) indicate the presence of the lone electron pair at the Sn atom, and the corresponding natural bond orbital was also found by the NBO analysis (occupancy 1.98 e).

The calculated first and second adiabatic electron affinities of **1** are very similar (−0.05 and −0.13 eV in terms of  $\Delta G$ ). This indicates the possibility of overlap of the two possible single-electron reduction waves of *trans-1*, resulting in one broad two-electron reduction wave which is observed experimentally by cyclic voltammetry. In accord, a close inspection of the broad reduction wave  $\text{I}^{\text{red}}$  (Figure 6a) reveals an ill-defined shoulder at a slightly less cathodic potential (*ca.* −0.8 V) than  $E_p^{\text{red}}$ . Hence, interestingly, although complex *trans-1* undergoes two sequential one-electron reductions centered at the phenylcarboxylate ligands, the final doubly reduced complex displays only the Sn atom in the reduced (+II) state. The overall 2e-reduction results in the  $\text{Sn}^{\text{IV}} \rightarrow \text{Sn}^{\text{II}}$  reduction which, however, occurs stepwise via the ligands reductions rather than by the direct reduction of the metal.

Let us consider now what occurs in the oxidation of the reduced species  $\text{I}^{2-}$ , i.e., upon scan reversal following the reduction wave  $\text{I}^{\text{red}}$ .

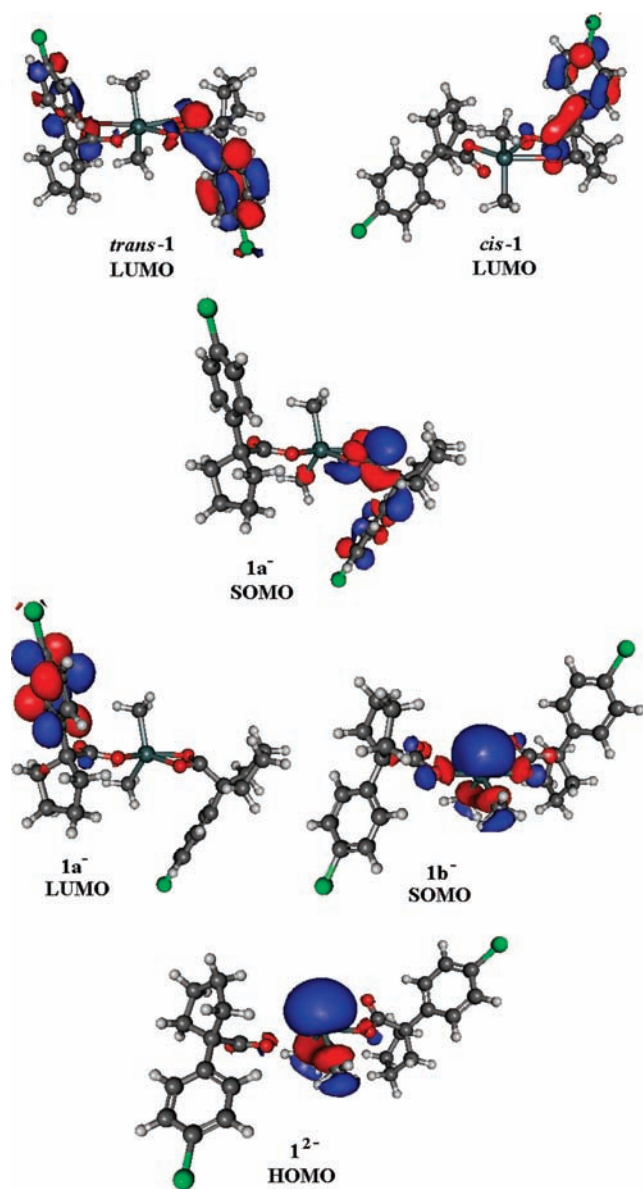
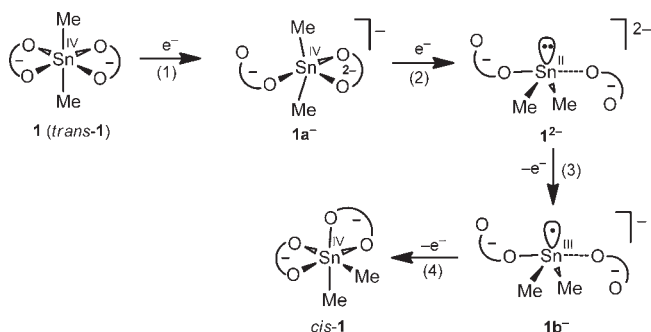


**Figure 7.** Plots of the frontier MOs of  $[\text{Me}_2\text{Sn}(\text{L})_2]$  (*trans*-1), reduced forms  $1\text{a}^-$  and  $1^{2-}$ , and reoxidized forms  $1\text{b}^-$  and *cis*-1.

The geometry optimization of the singly reduced species starting from the equilibrium geometry of  $1^{2-}$  resulted into another structure,  $1\text{b}^-$ , which is different from  $1\text{a}^-$  and more stable by 23.6 kcal/mol. Both  $\text{L}^-$  ligands in  $1\text{b}^-$  remain monodentate, the Me ligands keep the equatorial positions, and the polyhedron is still of a sawhorse (seesaw) type (Figure S3) (Scheme 1, third step). This structural type as well as the SOMO composition (Figure 7) and the NBO analysis indicate that the unpaired electron in  $1\text{b}^-$  is located on the metal which, thus, has the oxidation state +III (the spin density on the Sn atom is 0.72 e). Finally, the geometry optimization of **1** starting from the equilibrium structures of  $1\text{b}^-$  or  $1^{2-}$  revealed that the product of the oxidation of the reduced species is the *cis*-isomer of **1** (*cis*-1) (Scheme 1, fourth step) instead of the more stable (by 2.5 kcal/mol) initial *trans*-1. Thus, the back oxidation of  $1^{2-}$  to **1** occurs via the pathway  $1^{2-} \rightarrow 1\text{b}^- \rightarrow \text{cis-1}$  which is different from the route of the reduction of *trans*-1 (*trans*-1  $\rightarrow 1\text{a}^- \rightarrow 1^{2-}$ ).<sup>75</sup>

**Scheme 1.** Simplified Representation of the Electronic and Structural Rearrangements Occurring upon Two Sequential One-Electron Reductions of  $[\text{Me}_2\text{Sn}(\text{L})_2]$  (**1**)<sup>a</sup> and Following Oxidations<sup>b</sup>



<sup>a</sup> CV reduction wave  $\text{I}^{\text{red}}$ . <sup>b</sup> CV oxidation waves  $\text{I}^{\text{ox}}$  and  $\text{II}^{\text{ox}}$  in the anodic sweep upon scan reversal after  $\text{I}^{\text{red}}$  wave.

**Table 2.** Inhibition [%] of Compounds 1–6 [dose level of 10.00  $\mu\text{M}$ ] against Human Tumor Cells

compd	HL-60	BGC-823	Bel-7402	KB
1	7.8		16.4	10.9
2	22.4	6.7	16.4	8.7
3	34.0	89.4 <sup>a</sup>	88.8 <sup>b</sup>	39.2
4	8.6	12.6	12.8	
5	21.5	17.4	13.3	24.4
6	26.9	12.7	7.1	19.5
HL	1.2	4.5		
cisplatin	56.5	90.8 <sup>c</sup>	79.1 <sup>d</sup>	69.4

<sup>a</sup>  $\text{IC}_{50} = 4.9 \mu\text{M}$ . <sup>b</sup>  $\text{IC}_{50} = 5.2 \mu\text{M}$ . <sup>c</sup>  $\text{IC}_{50} = 6.5 \mu\text{M}$ . <sup>d</sup>  $\text{IC}_{50} = 8.1 \mu\text{M}$ .

Structural rearrangements and bond cleavages induced by electron transfer are well documented,<sup>37,76–83</sup> and those observed in this study are a rare combination of the following types: (i) cathodically induced metal–ligand bond cleavage and *trans*/*cis* isomerization; (ii) anodically induced metal–ligand bond formation.

**3.5. Anticancer Activity of 1–6.** All the synthesized compounds were screened for the preliminary in vitro anticancer activity against four different human cell lines: a promyelocytic leukemia cell line (HL-60), a hepatocellular carcinoma cell line (Bel-7402), a gastric carcinoma cell line (BGC-823), and nasopharyngeal carcinoma (KB), at three different concentrations. Because most of compounds showed inhibition activity at concentration of  $>10 \mu\text{M}$ , we herein merely list the biological results at the concentration of  $10 \mu\text{M}$  in Table 2 for the purpose of discussing any eventual structure–activity relationships.

Among the six organotin(IV) complexes checked, only compound **3** exhibits a strong activity against Bel-7402 and BGC-823, being even slightly more active than cisplatin, which is clinically widely used. Hence, the  $\text{IC}_{50}$  values for **3** and cisplatin are 5.2 and  $8.1^{38} \mu\text{M}$  (for Bel-7402), and 4.9 and  $6.5^{38} \mu\text{M}$  (for BGC-823), respectively.

On the basis of the data analysis, possible structure–activity relationships could be outlined as follows: (i) As observed in previous studies,<sup>1,9,18–20,84,85</sup> the organo-ligand R appears to

play an important role. Indeed, the di-*n*-butyltin complex exhibits the strongest antitumor activity, while the diorganotin derivatives with a too short (methyl) or a too long (*n*-octyl) carbon chain length exhibit very low activities. The activity of the diphenyltin complex (**5**) is also very weak, although usually better than those of dimethyltin (**1**), diethyltin (**2**), and di-*n*-octyltin (**4**). Hence, for this class of diorganotin complexes, the activity follows the order  ${}^n\text{Bu} > \text{Ph} \geq \text{Et} \geq {}^n\text{Oct}$ , Me for most of the tumor cells. (ii) The hexanuclear phenyltin compound (**6**) shows a weak activity against nearly all the tumor cells, indicating that a polynuclear character, *per se*, does not result in a high biological activity for organotin compounds. Probably, for **6**, the high coordination number and steric hindrance around tin are important factors for the weak activities, which limit the access of tin to the target. (iii) In comparison with other diorganotin(IV) carboxylate complexes,<sup>86,87</sup> this class of compounds shows lower antitumor activity against HL-60 and KB cell lines. However, for the dibutyltin(IV) derivatives, **3** is more active than many diorganotin(IV) hydroxamates<sup>18–20,85</sup> against BGC-823 and Bel-7402 cell lines.

#### 4. CONCLUSIONS

A series of mononuclear diorganotin(IV) compounds and a hexanuclear monophenyltin(IV) complex, all of them bearing 1-(4-chlorophenyl)-1-cyclopentanecarboxylate, were isolated and structurally characterized. Changes of the organo group and of the metal nuclearity lead to differences in both the antitumor activity and the reduction potential. [ ${}^n\text{Bu}_2\text{SnL}_2$ ] (**3**) is the most cytotoxic compound which is highly active against two tumor cell lines (BGC-823 and Bel-7402).

For the series of directly comparable mononuclear diorganotin complexes (**1–5**), the antitumor activity tends to follow the order  $3 ({}^n\text{Bu}) > 5 (\text{Ph}) \geq 2 (\text{Et}) \geq 4 ({}^n\text{Oct})$ ,  $1 (\text{Me})$ , whereas the reduction potential ( $E_p^{\text{red}}$ ) varies according to the order  $5 > 3 > 2 > 1 > 4$ . Hence, the higher activities are displayed by compounds (**3**, **5**) that are easier to reduce, while those that are more difficult to reduce (**1**, **4**) exhibit the lowest activities. Moreover, the reduction potentials of our complexes, in particular that of the most active one (**3**,  $E_p^{\text{red}} = -1.04 \text{ V}$  vs SCE =  $-0.78 \text{ V}$  vs. NHE), lie within the range of those of other metal-based antitumor complexes, e.g., of Ru(III)<sup>29</sup> or Pt(IV),<sup>29,88,89</sup> that activated by reduction in the tumor cells that are known to display a stronger reductive medium than the normal healthy cells.

This suggests the conceivable activation of the diorganotin(IV) drug by reduction and the electrochemical/theoretical studies disclose the involvement, in the reduction process, of structural rearrangements that can promote the action of the drug, *i.e.*, (i) the cleavage of Sn–O(ligand) bonds (generating coordinative unsaturation) and (ii) a geometrical *trans*-to-*cis* isomerization (it is noteworthy the common higher activity of the *cis* isomer than that the *trans* one e.g. in the conventional Pt drugs). Both features (i and ii), induced by reduction, can favor the drug attack to the target species.

Nevertheless, the hexanuclear complex **6** (the easiest one to reduce) does not follow this trend, possibly on account of the above-mentioned structural features that hamper its bioactivity. Moreover, since our study concerns only a few compounds, a correlation between  $E_p$  and inhibition values cannot yet be claimed. Further investigation of a much greater number of organotin(IV) compounds should be carried out

before any clear redox potential-activity relationship can be proposed.

#### ■ ASSOCIATED CONTENT

Supporting Information. Additional table and figures. This material is available free of charge via the Internet at <http://pubs.acs.org>.

#### ■ AUTHOR INFORMATION

##### Corresponding Author

\*E-mail: [pombeiro@ist.utl.pt](mailto:pombeiro@ist.utl.pt). Fax: +351 218464455.

#### ■ ACKNOWLEDGMENT

This work has been partially supported by the Foundation for Science and Technology (FCT) (its PEst-OE/QUI/UI0100/2011 project, and Grant SFRH/BPD/44773/2008), Portugal, and the New Drug Development Programme from the Ministry of Science and Technology of China (No. 2009ZX09103-104).

#### ■ REFERENCES

- (1) Pizarro A. M.; Hablemariam A.; Sadler P. J. Activation Mechanisms for Organometallic Anticancer Complexes; In *Med. Organomet. Chem.*; Topics in Organometallic Chemistry; Jaouen, G., Metzler-Nolte, N., Eds.; **2010**, *32*, 21–46.
- (2) Gielen, M.; Tiekink, E. R. T. *Metallotherapeutic Drugs and Metal-Based Diagnostic Agents: The Use of Metals in Medicine*; John Wiley & Sons Ltd.: New York, 2005; pp 421–435.
- (3) Gasser, G.; Otto, I.; Metzler-Nolte, N. *J. Med. Chem.* **2011**, *54*, 3–25.
- (4) Gianferrara, T.; Bratsos, I.; Alessio, E. *Dalton Trans.* **2009**, *37*, 7588–7598.
- (5) LaMaryet, M.; Hader, A. A. *Annu. Rep. Prog. Chem., Sect. A: Inorg. Chem.* **2009**, *105*, 505–524.
- (6) Hadjikakou, S. K.; Hadjiliadis, N. *Coord. Chem. Rev.* **2009**, *253*, 235–249.
- (7) Tabassum, S.; Pettinari, C. *J. Organomet. Chem.* **2006**, *691*, 1761–1766.
- (8) Pellerito, C.; Nagy, L.; Pellerito, L.; Szorcisk, A. *J. Organomet. Chem.* **2006**, *691*, 1733–1747.
- (9) Gielen, M.; Biesemans, M.; Willem, R. *Appl. Organomet. Chem.* **2005**, *19*, 440–450.
- (10) Pellerito, L.; Nagy, L. *Coord. Chem. Rev.* **2002**, *224*, 111–150.
- (11) Michael, J. C.; Fuchun, Z.; Dominic, R. F. *Chem. Rev.* **1999**, *2511–2533*.
- (12) Gielen, M. *Coord. Chem. Rev.* **1996**, *151*, 41–51.
- (13) Sadler, P. J. *Adv. Inorg. Chem.* **1991**, *36*, 1–48.
- (14) Tiekink, E. R. T. *Crit. Rev. Oncol./Hematol.* **2002**, *42*, 217–224.
- (15) Guo, Z.; Sadler, P. J. *Angew. Chem., Int. Ed.* **1999**, *38*, 1512–1531.
- (16) Xanthopoulou, M. N.; Hadjikakou, S. K.; Hadjiliadis, N.; Milaeva, E. R.; Gracheva, J. A.; Tyurin, V.-Y.; Kourkoumelis, N.; Christoforidis, K. C.; Metsios, A. K.; Karkabounas, S.; Charalabopoulos, K. *Eur. J. Med. Chem.* **2008**, *43*, 327–335.
- (17) Shang, X. M.; Cui, J. R.; Wu, J. Z.; Pombeiro, A. J. L.; Li, Q. S. *J. Inorg. Biochem.* **2008**, *102* (4), 901–909.
- (18) Li, Q.; Guedes da Silva, M. F. C.; Pombeiro, A. J. L. *Chem.—Eur. J.* **2004**, *10*, 1456–1462.
- (19) Li, Q.; Guedes da Silva, M. F. C.; Zhao, J. H.; Pombeiro, A. J. L. *J. Organomet. Chem.* **2004**, *689*, 4584–4591.
- (20) Nath, M.; Pokharia, S.; Song, X.; Eng, G.; Gielen, M.; Kemmer, M.; Biesemans, M.; Willem, R.; de Vos, D. *Appl. Organomet. Chem.* **2003**, *17*, 305–314.
- (21) Gielen, M.; Biesemans, M.; de Vos, D.; Willem, R. *J. Inorg. Biochem.* **2000**, *79*, 139–145.



- (22) de Vos, D.; Willem, R.; Gielen, M.; van Wingerden, K. E.; Nooter, K. *Met.-Based Drugs* **1998**, *5*, 179–188.
- (23) Gielen, M.; Dalil, H.; Mahieu, B.; de Vos, D.; Biesemans, M.; Willem, R. *Met.-Based Drugs* **1998**, *5*, 275–278.
- (24) Tiekink, E. R. T.; Gielen, M.; Bouhdid, A.; Willem, R.; Bregadze, V. I.; Ermanson, L. V.; Glazun, S. A. *Met.-Based Drugs* **1997**, *4*, 75–80.
- (25) Jancso, A.; Nagy, L.; Moldrheim, E.; Sletten, E. *J. Chem. Soc., Dalton Trans.* **1999**, 1587–1594.
- (26) Li, Q.; Yang, P.; Wang, H.; Guo, M. *J. Inorg. Biochem.* **1996**, *64*, 181–195.
- (27) Barbieri, R.; Silvestri, A.; Giuliani, A. M.; Piro, V.; Di Simone, F.; Madonia, G. *J. Chem. Soc., Dalton Trans.* **1992**, 585–590.
- (28) Shang, X. M.; Wu, J. Z.; Li, Q. S. *Chin. J. Chem.* **2008**, *26*, 627–630.
- (29) Reisner, E.; Arion, V. B.; Keppler, B. K.; Pombeiro, A. J. L. *Inorg. Chim. Acta* **2008**, *361*, 1569–1583.
- (30) Kowol, C. R.; Reisner, E.; Chiorescu, I.; Arion, V. B.; Galanski, M.; Deubel, D. V.; Keppler, B. K. *Inorg. Chem.* **2008**, *47*, 11032–11047.
- (31) Cebrian-Losantos, B.; Reisner, E.; Kowol, C. R.; Roller, A.; Shova, S.; Arion, V. B.; Keppler, B. K. *Inorg. Chem.* **2008**, *47*, 6513–6523.
- (32) Groessel, M.; Reisner, E.; Hartinger, C. G.; Eichinger, R.; Semenova, O.; Timerbaev, A. R.; Jakupec, M. A.; Arion, V. B.; Keppler, B. K. *J. Med. Chem.* **2007**, *50*, 2185–2193.
- (33) Jakupec, M. A.; Reisner, E.; Eichinger, A.; Pongratz, M.; Arion, V. B.; Galanski, M.; Hartinger, C. G.; Keppler, B. K. *J. Med. Chem.* **2005**, *48*, 2831–2837.
- (34) Reisner, E.; Arion, V. B.; Eichinger, A.; Kandler, N.; Giester, G.; Pombeiro, A. J. L.; Keppler, B. K. *Inorg. Chem.* **2005**, *44*, 6704–6716.
- (35) Hall, M. D.; Amjadi, S.; Zhang, M.; Beale, P. J.; Hambley, T. W. *J. Inorg. Biochem.* **2004**, *98*, 1614–1624.
- (36) Saxena, A. K.; Huber, F. *Coord. Chem. Rev.* **1989**, *95*, 109–123.
- (37) Juranić, I. O.; Drakulić, B. J.; Petrović, S. D.; Mijin, D. Z.; Stanković, M. V. *Chemosphere* **2006**, *62*, 641–649.
- (38) Zhang, J.; Li, L.; Wang, L.; Zhang, F.; Li, X. *Eur. J. Med. Chem.* **2010**, *45*, 5337–5344.
- (39) Pombeiro, A. J. L.; da Silva, M. F. C. G.; Lemos, M. A. N. D. A. *Coord. Chem. Rev.* **2001**, *219–221*, 53–80.
- (40) APEX2 & SAINT; Bruker, AXS Inc.: Madison, WI, 2004.
- (41) Sheldrick, G. M. *Acta Crystallogr., Sect. A* **1990**, *A46*, 467–473.
- (42) Sheldrick, G. M. *Acta Crystallogr., Sect. A* **2008**, *A64*, 112–122.
- (43) Farrugia, L. J. *J. Appl. Crystallogr.* **2003**, *36*, 141–145.
- (44) Denizot, F.; Lang, R. *J. Immunol. Methods* **1986**, *89*, 271–277.
- (45) Skehan, P.; Storeng, R.; Scudiero, D.; Monks, A.; McMahon, J.; Vistica, D.; Warren, J. T.; Bokesch, H.; Kenney, S.; Boyd, M. R. *J. Natl. Cancer Inst.* **1990**, *82*, 1107–1112.
- (46) Schempp, C. M.; Kirkin, V.; Simon-Haarhaus, B.; Kersten, A.; Kiss, J.; Termeer, C. C.; Gilb, B.; Kaufmann, T.; Borner, C.; Sleeman, P. J.; Simon, J. C. *Oncogene* **2002**, *21*, 1242–1250.
- (47) Becke, A. D. *J. Chem. Phys.* **1993**, *98*, 5648–5652.
- (48) Lee, C.; Yang, W.; Parr, R. G. *Phys. Rev. B* **1988**, *37*, 785–789.
- (49) Frisch, M. J.; Trucks, G. W.; Schlegel, H. B.; Scuseria, G. E.; Robb, M. A.; Cheeseman, J. R.; Zakrzewski, V. G.; Montgomery, J. A.; Stratmann, R. E., Jr.; Burant, J. C.; Dapprich, S.; Millam, J. M.; Daniels, A. D.; Kudin, K. N.; Strain, M. C.; Farkas, O.; Tomasi, J.; Barone, V.; Cossi, M.; Cammi, R.; Mennucci, B.; Pomelli, C.; Adamo, C.; Clifford, S.; Ochterski, J.; Peterson, G. A.; Ayala, P. Y.; Cui, Q.; Morokuma, K.; Malick, D. K.; Rabuck, A. D.; Raghavachari, K.; Foresman, J. B.; Cioslowski, J.; Ortiz, J. V.; Baboul, A. G.; Stefanov, B. B.; Liu, G.; Liashenko, A.; Piskorz, P.; Komaromi, I.; Gomperts, R.; Martin, R. L.; Fox, D. J.; Keith, T.; Al-Laham, M. A.; Peng, C. Y.; Nanayakkara, A.; Challacombe, M.; Gill, P. M. W.; Johnson, B.; Chen, W.; Wong, M. W.; Andres, J. L.; Gonzalez, C.; Head-Gordon, M.; Replogle, E. S.; Pople, J. A. *Gaussian 98, revision A.9*; Gaussian, Inc.: Pittsburgh PA, 1998.
- (50) Bergner, A.; Dolg, M.; Kuechle, W.; Stoll, H.; Preuss, H. *Mol. Phys.* **1993**, *80*, 1431–1441.
- (51) Reed, A. E.; Curtiss, L. A.; Weinhold, F. *Chem. Rev.* **1988**, *88*, 899–926.
- (52) Dakternieks, D.; Basu Baul, T. S.; Dutta, S.; Tiekink, E. R. T. *Organometallics* **1998**, *17*, 3058–3062.
- (53) (a) Yin, H. D.; Wang, Q. B.; Xue, S. C. *J. Organomet. Chem.* **2005**, *690*, 435–440. (b) Kang, W.; Wu, X.; Huang, J. *J. Organomet. Chem.* **2009**, *694*, 2402–2408.
- (54) Tzimopoulos, D.; Sanidas, I.; Varvogli, A.-C.; Czapik, A.; Gdaniec, M.; Nikolakaki, E.; Akrivos, P. D. *J. Inorg. Biochem.* **2010**, *104*, 423–430.
- (55) Gielen, M.; Khloufi, A. E.; Biesemans, M.; Kayser, F.; Willem, R. *Appl. Organomet. Chem.* **1993**, *7*, 201–206.
- (56) Howard, W. F.; Crecey, R. W.; Nelson, W. H. *Inorg. Chem.* **1985**, *24*, 2204–2208.
- (57) Holeccek, J.; Nádvorník, M.; Handlír, K.; Lycka, A. *J. Organomet. Chem.* **1986**, *315*, 299–308.
- (58) Otera, J. *J. Organomet. Chem.* **1981**, *221*, 57–61.
- (59) Otera, J.; Kusaba, A.; Hinoishi, T.; Kawasaki, Y. *J. Organomet. Chem.* **1982**, *228*, 223–228.
- (60) Teoh, S. G.; Ang, S. H.; Loot, E. S.; Keok, C. A.; Tea, S. B.; Declercq, J. P. *J. Organomet. Chem.* **1996**, *523*, 75–78.
- (61) Chandrasekhar, V.; Day, R. D.; Holmes, J. M.; Holmes, R. R. *Inorg. Chem.* **1988**, *27*, 958–964.
- (62) Chandrasekhar, V.; Nagendran, S.; Banzal, S.; Kozee, M. A.; Powell, D. R. *Angew. Chem., Int. Ed.* **2000**, *39*, 1833–1835.
- (63) Chandrasekhar, V.; Nagendran, S.; Bansal, S.; Cordes, A. W.; Vij, A. *Organometallics* **2002**, *21*, 3297–3300.
- (64) Chandrasekhar, V.; Thirumoorathi, R. *Eur. J. Inorg. Chem.* **2008**, 4578–4585.
- (65) Pombeiro, A. J. L. *J. Organomet. Chem.* **2005**, *690*, 6021–6040.
- (66) Pombeiro, A. J. L. *Eur. J. Inorg. Chem.* **2007**, 1473–1482.
- (67) Pombeiro, A. J. L. Redox Potential-Structure Relationships in Coordination Compounds. In *Encyclopedia of Electrochemistry*; Bard, A. J., Stratmann, M., Eds.; Vol. 7A, Inorganic Chemistry; Scholz, F., Pickett, C. J., Eds.; Wiley-VCH: New York, 2006; Chapter 3, pp 77–108.
- (68) Lever, A. B. P. *Inorg. Chem.* **1991**, *30*, 1980–1985.
- (69) Lever, A. B. P. *Inorg. Chem.* **1991**, *29*, 1271–1285.
- (70) Lever, A. B. P. *Coord. Chem. Rev.* **2010**, *254*, 1397–1405.
- (71) Kalinina, D.; Dares, C.; Kaluarachchi, H.; Potvin, P. G.; Lever, A. B. P. *Inorg. Chem.* **2008**, *47*, 10110–10126.
- (72) Almeida, S. S. P. R.; Pombeiro, A. J. L. *Organometallics* **1997**, *16*, 4469–4478.
- (73) Silva, M. E. N. P. R. A.; Pombeiro, A. J. L.; da Silva, J. J. R. F.; Hermann, R.; Deus, N.; Castilho, T. J.; da Silva, M. F. C. G. *J. Organomet. Chem.* **1991**, *421*, 75–90.
- (74) Pombeiro, A. J. L. *Inorg. Chim. Acta* **1985**, *103*, 95–103.
- (75) The  $1a^- \rightarrow 1b^-$  isomerization at the stage of the reduction should be significantly slower than the second electron addition to  $1a^-$  leading to  $1^{2-}$ .
- (76) *Trends in Molecular Electrochemistry*; Pombeiro, A. J. L., Amatore, C., Eds.; Marcel Dekker Inc.: New York, 2004; p 552.
- (77) Connelly, N. G.; Geiger, W. E. *Chem. Rev.* **1996**, *96*, 877–910.
- (78) Zanello, P. *Inorganic Chemistry, Theory, Practice and Application*; Royal Society of Chemistry: Cambridge, U.K., 2003; p 615.
- (79) Astruc, D. *Electron Transfer and Radical Processes in Transition-Metal Chemistry*; VCH: New York, 1995, 630.
- (80) Martins, N. C. T.; Guedes da Silva, M. F. C.; Wanke, R.; Pombeiro, A. J. L. *Dalton Trans.* **2009**, 4772–4777.
- (81) Guedes da Silva, M. F. C.; da Silva, J. A. L.; Fraústo da Silva, J. J. R.; Pombeiro, A. J. L.; Amatore, C.; Verpeaux, J. N. *J. Am. Chem. Soc.* **1996**, *118*, 7568–7573.
- (82) Guedes da Silva, M. F. C.; Ferreira, C. M. P.; Fraústo da Silva, J. J. R.; Pombeiro, A. J. L. *J. Chem. Soc., Dalton Trans.* **1998**, 4139–4145.
- (83) Guedes da Silva, M. F. C.; Fraústo da Silva, J. J. R.; Pombeiro, A. J. L.; Amatore, C.; Verpeaux, J. N. *Inorg. Chem.* **1998**, *37*, 2344–2350.
- (84) Gielen, M. *Appl. Organomet. Chem.* **2002**, *16*, 481–494.
- (85) Shang, X. M.; Wu, J. Z.; Pombeiro, A. J. L.; Li, Q. S. *Appl. Organomet. Chem.* **2007**, *21*, 919–925.
- (86) Rehman, W.; Baloch, M. K.; Badshah, A.; Ali, S. *Spectrochim. Acta, Part A* **2006**, *65*, 689–694.

- (87) Zhou, Y.; Jiang, T.; Ren, S.; Yu, J.; Xia, Z. *J. Organomet. Chem.* **2005**, *690*, 2186–2190.
- (88) Ellis, L. T.; Er, H. M.; Hambley, T. W. *Aust. J. Chem.* **1995**, *48*, 793–806.
- (89) Hall, M. D.; Amjadi, S.; Zhang, M.; Beale, P. J.; Hambley, T. W. *J. Inorg. Biochem.* **2004**, *98*, 1614–1624.